


## Article

# Dual-Step Controlled Release of Berberine Hydrochloride from the Trans-Scale Hybrids of Nanofibers and Microparticles

Jianfeng Zhou <sup>1,†</sup>, Yelin Dai <sup>2,3,†</sup>, Junhao Fu <sup>1</sup>, Chao Yan <sup>1</sup>, Deng-Guang Yu <sup>1,\*</sup>  and Tao Yi <sup>4,\*</sup>

<sup>1</sup> School of Materials and Chemistry, University of Shanghai for Science and Technology, Shanghai 200093, China; 221550217@st.usst.edu.cn (J.Z.); 2035053109@st.usst.edu.cn (J.F.); 2026010226@st.usst.edu.cn (C.Y.)

<sup>2</sup> Wenqi Middle School, East Jiangchuan Road 980, Shanghai 200240, China; daiyelin2007@163.com

<sup>3</sup> High School Affiliated to Fudan University, Qingpu Campus, Longpu Road 500, Shanghai 201700, China

<sup>4</sup> Faculty of Health Sciences and Sports, Macao Polytechnic University, Macau 999078, China

\* Correspondence: ydg017@usst.edu.cn (D.-G.Y.); yitao@mpu.edu.mo (T.Y.)

† These authors contributed equally to this work.

**Abstract:** In this nano era, nanomaterials and nanostructures are popular in developing novel functional materials. However, the combinations of materials at micro and macro scales can open new routes for developing novel trans-scale products with improved or even new functional performances. In this work, a brand-new hybrid, containing both nanofibers and microparticles, was fabricated using a sequential electrohydrodynamic atomization (EHDA) process. Firstly, the microparticles loaded with drug (berberine hydrochloride, BH) molecules in the cellulose acetate (CA) were fabricated using a solution electrospinning process. Later, these microparticles were suspended into a co-dissolved solution that contained BH and a hydrophilic polymer (polypyrrolidone, PVP) and were co-electrospun into the nanofiber/microparticle hybrids. The EHDA processes were recorded, and the resultant trans-scale products showed a typical hybrid topography, with microparticles distributed all over the nanofibers, which was demonstrated by SEM assessments. FTIR and XRD demonstrated that the components within the hybrids were presented in an amorphous state and had fine compatibility with each other. In vitro dissolution tests verified that the hybrids were able to provide the designed dual-step drug release profiles, a combination of the fast release step of BH from the hydrophilic PVP nanofibers through an erosion mechanism and the sustained release step of BH from the insoluble CA microparticles via a typical Fickian diffusion mechanism. The present protocols pave a new way for developing trans-scale functional materials.

**Keywords:** dual-step release; berberine hydrochloride; hybrid; electrospinning; nanofibers; electrospinning; microparticle



**Citation:** Zhou, J.; Dai, Y.; Fu, J.; Yan, C.; Yu, D.-G.; Yi, T. Dual-Step Controlled Release of Berberine Hydrochloride from the Trans-Scale Hybrids of Nanofibers and Microparticles. *Biomolecules* **2023**, *13*, 1011. <https://doi.org/10.3390/biom13061011>

Academic Editors: Jayakumar Rajadas and Mustafeez Mujtaba Babar

Received: 15 May 2023

Revised: 15 June 2023

Accepted: 16 June 2023

Published: 18 June 2023



**Copyright:** © 2023 by the authors. Licensee MDPI, Basel, Switzerland. This article is an open access article distributed under the terms and conditions of the Creative Commons Attribution (CC BY) license (<https://creativecommons.org/licenses/by/4.0/>).

## 1. Introduction

As an advanced drug controlled release profile, dual-step release (or biphasic release) has its advantages of endowing a fast therapeutic action effect and a long time period of constant blood drug concentration for the patients' conveniences [1–7]. In general, the first phase fast or pulsatile release of a drug is able to promote the drug concentration in the blood to a therapeutic window. Later, the second phase release is realized through a sustained or extended manner, by which the drug blood concentration is kept within the therapeutic window [8–15]. Thus, their combination, on one hand, can accelerate the therapeutic action. On the other hand, it can reduce the oral administration times for an increased patients' compliance [16–19].

Berberine hydrochloride (BH), a popular biomolecule with broad functional performances, is a typical poorly water-soluble drug. It can be extracted from *Coptis chinensis* and belongs to a chemical drug purified from traditional Chinese medicine. BH has a broad antibacterial spectrum and has antibacterial effects on a variety of Gram-positive

and negative bacteria, including *hemolytic streptococci*, *Staphylococcus aureus*, *Vibrio cholera*, *Meningococci*, *Shigella dysentery bacilli*, *Typhoid bacilli*, and *Diphtheria bacilli* [20]. At a low concentration, it inhibits bacteria, while at a high concentration, it kills bacteria. BH also has certain inhibitory effects on influenza viruses, amoeba, leptospira, and certain skin fungi [21]. In vitro experiments confirmed that BH can enhance the phagocytic ability of white blood cells and the hepatic reticuloendothelial system. BH has a therapeutic effect on helicobacter, and can alleviate gastritis, gastric and duodenal ulcers. It is reported that BH can reduce the number of pili on the surface of the bacterial body, preventing bacteria from adhering to human cells and, thus, has the therapeutic functional performance [22]. BH has no cross resistance to penicillin, streptomycin, etc. However, the oral absorption of BH is very poor. Furthermore, it quickly enters various organs and tissues and distributed widely (mostly in the heart, bone, lung, and liver) after intramuscular injection, and the blood drug concentration is maintained to the level over the minimum inhibitory concentration for only a very short time period [23]. Thus, a frequent oral administration of the commercial BH products (such as tablets, capsules, and pills) is needed for the patients. Biphasic release of BH may benefit an improved therapeutic effect after oral administration.

During the past several decades, although many new excipients (including organic materials such as polymers and lipids, inorganic materials, their composites and hybrids [24–29]) and new strategies were frequently introduced into the pharmaceutical field for endowing the active ingredients a better therapeutic effect [30–34], the mainstream is still the traditional pharmaceutical excipients. This is because these excipients were demonstrated to be safe and compatible with organisms. Thus, for a certain drug, it is the material conversion methods that played their important roles in endowing an improved functional application. Particularly in this nano era, nano fabrication methods are continuously adopted by pharmacists to convert the drug molecules and excipient molecules to medicated nanoproductions for realizing the designed therapeutic effects [35,36]. Numerous examples can be found in the literature. One example is the electrospun nanofibers of traditional hydrophilic polymeric excipients (e.g., PVA, PVP, PEO, gelatin, and so on) for fast dissolution and therapeutic action of a poorly water-soluble drug [37–41]. Another example is the electrospayed microparticles and electrospun nanofibers of conventional insoluble or biodegradable polymeric excipients (e.g., CA, EC, PLA, PCL, PAN, and zein) for a designed drug sustained release profile [42–47].

Based on the hints from the above-mentioned studies, the present work investigated a combination of electrospinning and electrospaying (both belong to the technique of electrohydrodynamic atomization, EHDA) [48–50], by which a new type of hybrids consisting of both electrospun nanofibers and electrospayed microparticles were fabricated for providing a biphasic release of BH. The prepared hybrids were subjected to a series of characterizations including their morphology, the physical state and compatibility of the loaded components, and the in vitro drug controlled release profiles. Both the EHDA mechanism and drug biphasic release mechanism are proposed.

## 2. Materials and Methods

### 2.1. Materials

Berberine hydrochloride (BH, purity over 98%) was purchased from a local Laobaixing Drugstore (Shanghai, China). Cellulose acetate (Mw = 30,000) was bought from Aldrich. Polyvinylpyrrolidone K90 (Mw = 1,300,000) was purchased from Sigma-Aldrich Corp. (Shanghai, China) The solvents acetone, ethanol, Di-ChloroMethane (DCM) and N, N-Dimethylacetamide (DMAc) were obtained from Shanghai Fitst Shiji Factory (Shanghai, China). Water was double distilled just before use.

### 2.2. Fabrication Methods

Two different EHDA processes (i.e., a single-fluid blending electrospaying and a single-fluid blending electrospinning) were arranged in a sequential manner for preparing the hybrids of electrospun nanofibers and electrospayed microparticles.

According to literature [51], CA is soluble in a mixture of acetone/ethanol/DMAc with a volume ratio of 4:1:1. Meanwhile, the drug BH is soluble in DMAc; thus, a co-dissolving working fluid (Fluid 1, Table 1) containing CA and BH could be prepared for the single-fluid electrospaying process. After some pre-experiments, 15 g BH and 25 g CA were co-dissolved in 500 mL of the solvent mixture.

**Table 1.** Parameters for the EHDA processes.

No.	EHDA Process	Working Fluid	V (kV)	Experimental Conditions F (mL/h)	D (cm)	Drug Contents	Morpho-Logy
E1	Electrospaying	Fluid 1 <sup>a</sup>	20	1.0	20	20.0%	Particles
E2	Electrospinning	Fluid 2 <sup>b</sup>	8	2.0	20	10.0%	Fibers
E3	Sequential EHDA process	Fluid 3 <sup>c</sup>	12	2.0	20	14.3%	Hybrids

<sup>a</sup> Fluid 1: An amount of 5.0 g BH and 20.0 g CA were co-dissolved in 400 mL of the solvent mixture comprising acetone/ethanol/DMAc with a volume ratio of 4:1:1. <sup>b</sup> Fluid 2: An amount of 36.0 g PVP and 4.0 g BH were co-dissolved into 400 mL mixture of DCM and DMAc with a volume ratio of 9:1. <sup>c</sup> Fluid 3: An amount of 15.0 g microparticles E1 from electrospaying were suspended into 200 mL Fluid 2 uniformly through continuous stirring.

A homemade EHDA apparatus was exploited to conduct the electrospaying process. The experimental conditions include an applied voltage of 20 kV, a fluid flow rate of 1.0 mL/h, and a particle deposition distance of 20 cm from the nozzle of spinneret to the grounded collector. The environmental temperature and humidity were  $21 \pm 5$  °C and  $47 \pm 7\%$ , respectively.

An amount of 15.0 g microparticles E1 from electrospaying was suspended into 200 mL Fluid 2 (containing 36.0 g PVP and 4.0 g BH in 400 mL mixture of DCM and DMAc with a volume ratio of 9:1) uniformly through continuous stirring to form a suspension working fluid (Fluid 3, Table 1). During the electrospinning process, little sedimentation of the microparticles was observed, which should be attributed to the relatively lower density of electrospayed microparticles.

### 2.3. Characterization

#### 2.3.1. Morphology

The morphologies of the EHDA products were evaluated using a field-emission scanning electron microscope (SEM, Quanta FEG450, Hillsboro, OR, USA). The SEM pictures were used to estimate the average diameters of the nanofibers in about 100 places using the ImageJ software (National Institutes of Health, Bethesda, MD, USA). The sampling processes included fixing some powders E1 or a strip of E2 and E3 on a sample holder using a double-sided conductive adhesive, and a thin layer of Au was sprayed for 60 s before assessments under an applied voltage of 5.0 kV.

#### 2.3.2. Physical State and Compatibility among the Components

X-ray diffraction (XRD) tests were carried out using the Bruker X-ray Powder diffractometer (Bruker-AXS, Karlsruhe, Germany). The raw materials and their fiber mats were measured within a  $2\theta$  angle range of  $5^\circ$ – $60^\circ$ . The applied voltage and working current were 40 kV and 30 mA, respectively. The rotation speed was  $5^\circ$  per minute.

Fourier transform infrared (FTIR) analyses were implemented using a PerkinElmer FTIR Spectrometer (Spectrum 100, Billerica, MA, USA). The experiments were performed in range  $500$ – $4000$   $\text{cm}^{-1}$  with a resolution of  $2$   $\text{cm}^{-1}$ . The sampling for the solid materials included weighing 0.2 g of potassium bromide powder, grinding it with about 10 mg of the sample, pressing the mixture into solid tablets, and placing the tablets into the instrument for scanning.

#### 2.3.3. Functional Performances

The drug release profiles of the three EHDA products were assessed using the paddle method in accordance with the Chinese Pharmacopoeia (2020 Ed.). Approximately 200 mg of the EHDA products were placed into a vessel with 900 mL phosphate-buffered solution

(PBS, 0.1 M, pH = 7.0). The dissolution media were maintained at  $37 \pm 1$  °C and a rotation rate of 50 rpm. At predetermined time points, a volume of 5.0 mL aliquot was withdrawn and filtered through a 0.22  $\mu\text{m}$  membrane (Millipore, MA, USA). Five milliliters of fresh PBS was added to maintain a constant dissolution bulk volume. The amounts of BH released were measured at  $\lambda_{\text{max}} = 263$  nm using a UV-vis spectrophotometer (UV-2102PC, Unico Instrument Co. Ltd., Shanghai, China). A calibration equation was pre-determined for calculating the BH concentration. The experimental results were reported as mean  $\pm$  S.D. All experiments were repeated six times.

### 3. Results and Discussion

#### 3.1. The Sequential EHDA Process

EHDA processes are hydrodynamic atomization procedures that are initiated by an applied high voltage, and they are exploited to prepare solid products by taking advantages of the easy interactions between electrostatic energy and working fluids [52,53]. For electrospinning, the solid products are often nanofibers resulted from the continuous drawing of viscous polymer fluid jets [54–56]. For electrospaying, the solid products are typically microparticles that resulted from the fission and repelling of droplets [57]. Thus, based on the capabilities of these two EHDA processes, a new type of trans-scale hybrids can be conceived as Figure 1, and three kinds of EHDA products were fabricated according to the conditions listed in Table 1.

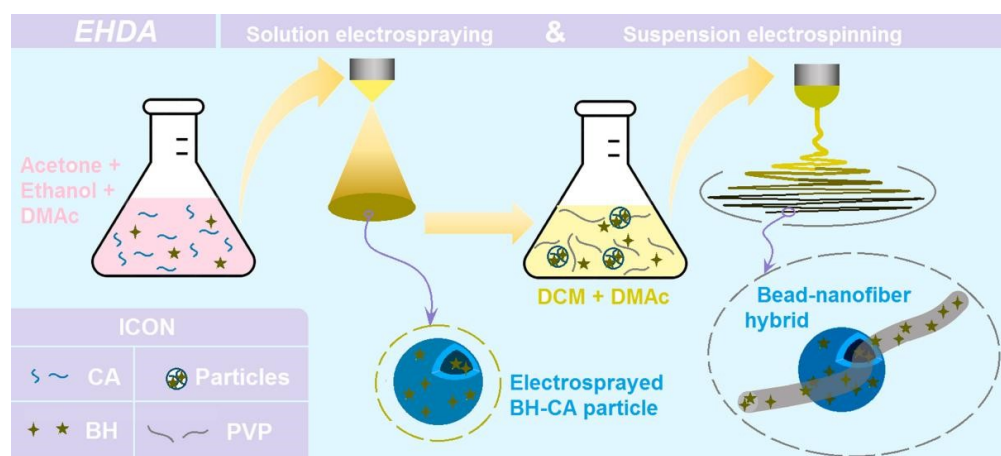


**Figure 1.** A diagram showing the fabrication procedures of the hybrids composed of the electrospun nanofibers and the electrospayed microparticles.

Firstly, the water-insoluble polymer CA and drug BH were co-dissolved into a solvent mixture containing acetone, ethanol, and DMAc with a volume ratio of 4:1:1. After some pre-experiments, the solid microparticles could be prepared through a single-step and straightforward electrospaying process. Later, these microparticles were dispersed into the co-dissolving solution containing PVP and BH in a solvent mixture containing DCM and DMAc with a volume ratio of 9:1. The CA particles did not dissolve in the solvent mixture. Thus, the working fluid was a suspension. After the electrospinning of the suspension, the hybrids containing both nanofibers of PVP and microparticles of CA were prepared, and the drug BH was distributed both in the nanofibers and also in the microparticles.

For a successful electrospinning process, the working fluid must be electrospinnable [58,59]. Thus, a relatively high polymer concentration is needed to keep enough physical entanglements of polymeric molecules in the working fluid, by which the electrostatic drawing can be resisted for elongating the fluid jets till the formation of nanofibers [60–62]. However, for a successful electrospaying process, the working fluid needs only to be solidifiable, i.e., the effective removal of organic solvents [63]. Thus, the polymer concentration is often lower than the electrospinnable one. Shown in Figure 2a is the typical digital picture taken from the electrospaying processes for fabricating the microparticles E1. At the

top of Taylor cone, an opposite cone can be observed for the Coulombic expansion. The “white” section region, indicated by a red arrow, was formed by the fast moving speed of the fast splitted droplets. As the droplets splitted and reduced their sizes and weights, their movings were decelerated, which can be recorded by a digital camera (30 frames per second). The PVP-BH solution had fine electrospinnability; a typical working process is given in Figure 2b, by which the composite nanofibers E2 were fabricated. Figure 2c exhibits the typical suspension electrospinning process for producing hybrids E3.

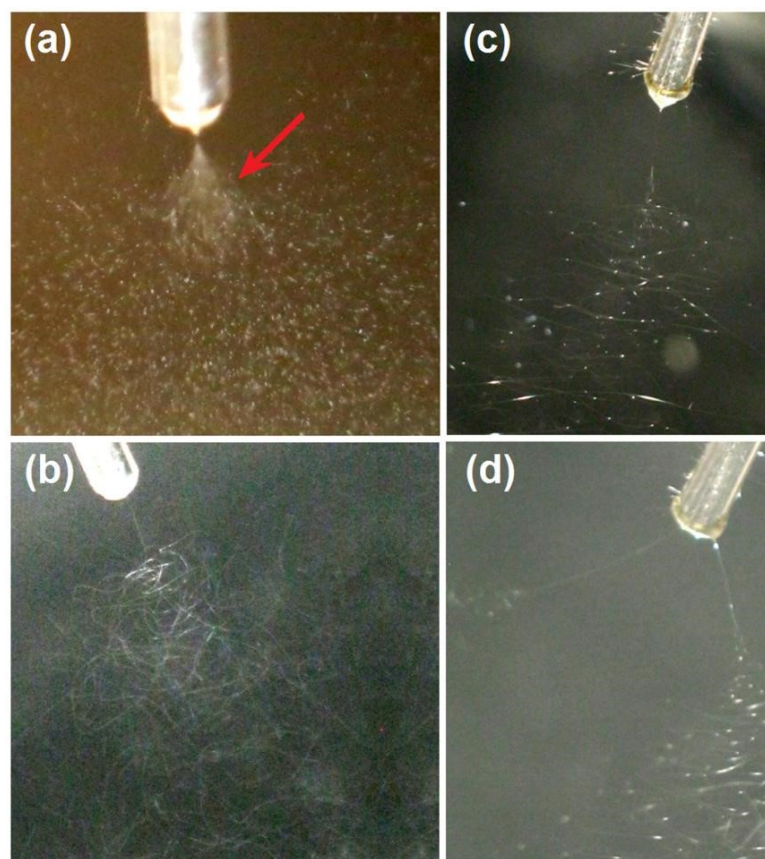


**Figure 2.** Digital pictures taken from the different EHDA working processes: (a) a typical electro-spraying process for fabricating the microparticles E1, the red arrow indicates a splitted and fast moving region; (b) a typical solution electrospinning process for creating the nanofibers E2; (c) a typical suspension electrospinning process for producing hybrids of E3; (d) an abnormal EHDA process when treating the suspension under a super high applied voltage.

The comparison between Figure 2b,c can tell the influence of the added CA microparticles on the electrospinning processes. Although under the same experimental conditions (a fixed applied voltage, flow rate, and a collected distance of 12 kV, 2.0 mL/h, and 20 cm, respectively), the three sections (Taylor cone, straight fluid jet, and bending and whipping region [64–67]) had significant differences. The Taylor cone and straight fluid jet of the treated suspension had a larger volume and a longer size than those of treated PVP solution. Apparently, the “large” weight of microparticles played their role in enlarging the Taylor cone and elongating the straight fluid jet. Furthermore, in the bending and whipping process of the unstable regions, it was clear that the bright dots, formed by the microparticles, were always there from the end of straight fluid jet to the deposition just above the collector. Meanwhile, the suspension jets movings showed the unsmooth polygonal lines, different with the smooth and continuous lines of solution jets movement trajectory. Still, the microparticles clung on the jets resulted in these complex phenomena. During the electrospinning of suspension for fabricating hybrids E3, the fluid jets were

more easily separated when a small elevation of the applied voltage to 15 kV. A typical record is shown in Figure 2d. After separation into two branches, the branch that contained more microparticles mainly moved downwards, owing to the presence of microparticles. Meanwhile, the easy aggregation of electric charges on the surface of microparticles should be also a reason for easy separation under a higher voltage. Thus, keeping a suitable applied voltage can benefit a higher quality of EHDA hybrids in terms of the uniform distribution of microparticles within the nanofibers. During all the processes, clogging of spinneret was seldom observed. In this work, two different kinds of EHDA processes were combined. Along this way, many other laboratory or even industrial techniques (such as supercritical technology and three-dimensional printing) can be combined with EHDA to develop novel materials conversion methods [68–70].

### 3.2. The Morphologies of the Resultant Products

The morphologies of the different EHDA products are included in Figure 3. Interestingly, there were many satellites around the electrospayed microparticles E1 (Figure 3a). For the application of drug sustained release, these satellites may be a negative factor due to the extremely small size and correspondingly the short routes for the loaded drug molecules diffusion from them to the bulk solutions. Just as anticipated, the electrospun BH-PVP nanofibers E2 had fine linear morphology without any discerned beads or spindles (Figure 3b). Meanwhile, an enlarged image in the up-right inset of Figure 3b indicates that these nanofibers had a very smooth surface without the possible drug particles formed by phase separation during the storage process. The electrospun hybrids from the suspensions exhibited a typical “mixture” of beads or spindles and nanofibers, as indicated by Figure 3c,d.

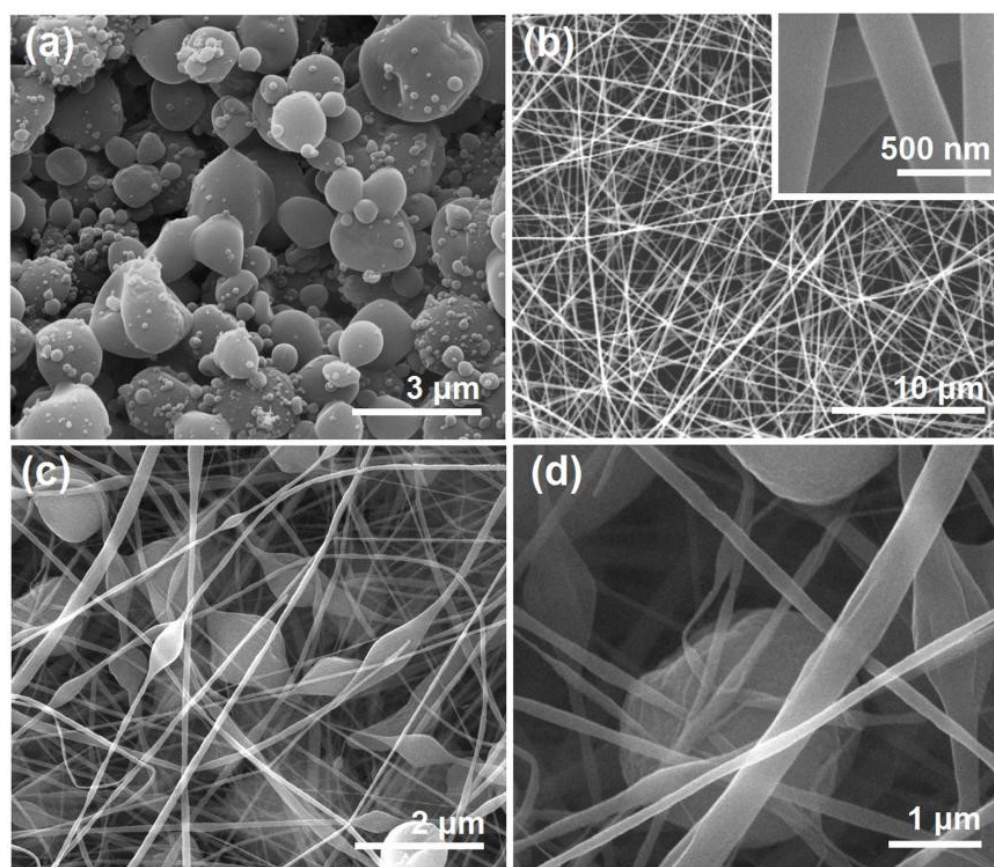


**Figure 3.** SEM images of the resultant products: (a) microparticles E1; (b) nanofibers E2, the up-right inset shows an enlarged image; (c) hybrids E3; (d) an enlarged image of hybrids E3.

The sizes and size distributions of these EHDA products were estimated using ImageJ software. All the results are shown in Figure 4. The average diameters of nanofibers E2 were  $330 \pm 60$  nm (Figure 4a). In sharp contrast, the diameters of the nanofiber sections in the electrospun hybrids E3 were only  $170 \pm 80$  nm (Figure 4b). The difference was a direct result of the added microparticles, whose presence should increase the drawing effects on the moving fluid jets and, in turn, a significant reduction in the nanofibers' diameter. The electrospayed microparticles E2 had an average diameter of  $2.89 \pm 0.53$   $\mu$ m (Figure 4c). In contrast, the diameter of particular sections in electrospun hybrids E3 was  $2.41 \pm 0.67$   $\mu$ m (Figure 4d), showing a slight reduction in the average size. This indicates that the re-dispersing of microparticles E1 in the solvent mixture of DCM and DMAc for preparing the suspension working fluid may result in a little influence on their final morphology and size. Although CA is insoluble in DCM and DMAc, the drug BH distributed on the surface of microparticles may re-dissolve into the suspensions and build a dynamic balance between the surfaces of microparticles and the bulk suspensions.

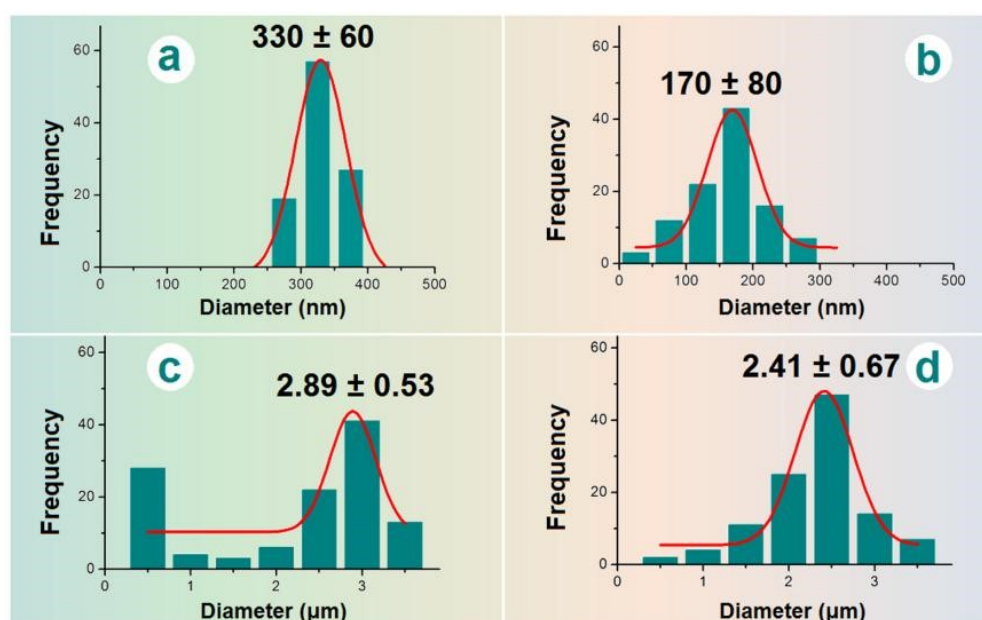


**Figure 4.** The average diameters of EHDA products: (a) nanofibers E2; (b) the nanofibers of hybrids E3; (c) microparticles E1; (d) the microparticles of hybrids E3.

Although there is no general theory for instructing the implementation of EHDA processes, there are abundant suggested mechanisms in the literature for the treatment of a certain working fluid, both for electrospinning and electrospaying. Those mechanisms are important for the continuous and robust production and duplication of the EHDA products. Meanwhile, as more and more EHDA products are going into the commercial markets, these mechanisms for optimizing the production processes, and other related issues such as energy-saving, safety implementation, and environmental friendliness and projecting their places for the final social benefits and a better people life [71–74]. In this work, the mechanism for the strange phenomenon of many satellites is diagrammed in Figure 5. In the left part, a whole electrospaying process is sketched, i.e., a Taylor one, to a convergent point, and later to the Coulombic explosion region, in which the droplets were continuously splitted and reduced, until the formation and deposition of solid particles on the collector.

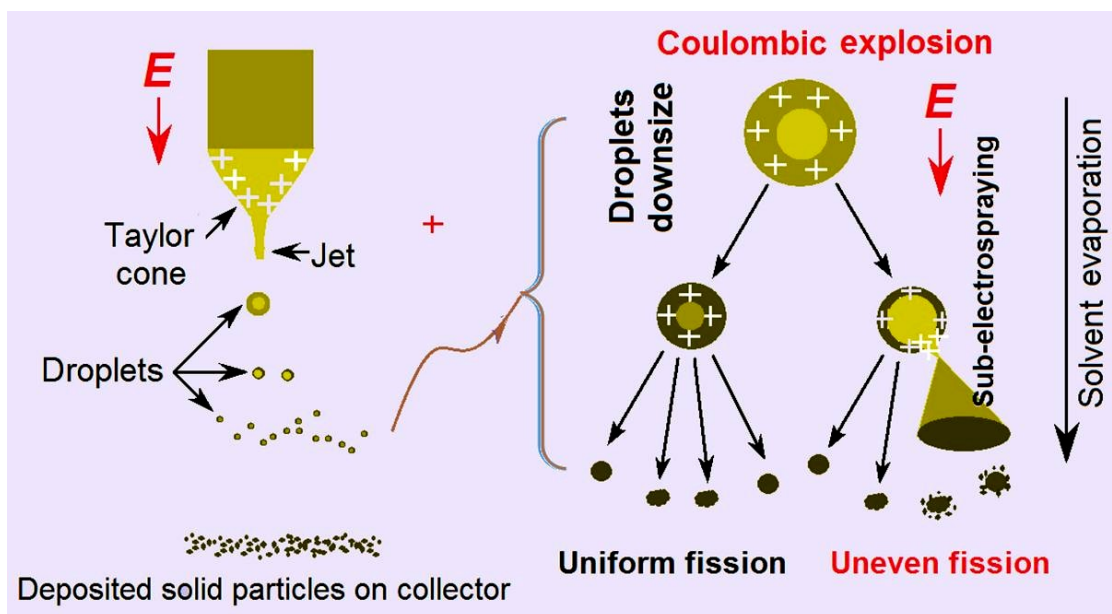


**Figure 5.** The EHDA mechanism for the formation of satellites around the electrospayed microparticles.

In the right part of Figure 5, two different fission processes are sketched. One kind was the uniform fission, by which the final electrospayed particles were generated, as indicated in Figure 3a, where the surfaces of microparticles are smooth. The other kind was uneven fission, by which many satellites were formed during the electrospaying processes and were around the electrospayed microparticles (Figure 3a). Their diameters were estimated to be several decades nanometers. In the electrospaying solution, the three solvents acetone, ethanol, and DMAc had their own main uses. CA is soluble in acetone and BH is soluble in DMAc. Although ethanol is a non-solvent for both BH and CA, it is useful for keeping the stretching state of CA molecules and, in turn, for promoting a stable and robust EHDA process. However, these solvents have different boiling points (56 °C, 78 °C, and 164 °C for acetone, ethanol, and DMAc, respectively) and different volatility. During the Coulombic explosion processes, it was possible that some droplets had more DMAc and kept a longer time period of the fluid state. Meanwhile, the surface charges may have different densities. Under these conditions, some sub-electrospraying processes may occur, by which the satellites are formed around the microparticles.

### 3.3. The Physical State and Compatibility

XRD patterns of the raw materials (CA, PVP, and BH) and their EHDA products (hybrids E3, nanofibers E2, and their combinations) are included in Figure 6. Just as anticipated, BH had many sharp Bragg peaks in its pattern due to the crystalline state of the original powders. In contrast, the hydrophilic polymer PVP K90 and insoluble polymer CA were all amorphous materials and, thus, only humped on their XRD patterns. The three EHDA products, i.e., the electrospayed microparticles E1, the electrospun nanofibers E2, and the electrospun hybrids E3, showed no any sharp peaks in their patterns. These phenomena suggested that the drug BH was converted into amorphous composites in all of them after the electrospaying or electrospinning processes. An amorphous state of the drug is favorable for its dissolution and the manipulation of a certain controlled release profile from the matrices [75,76].



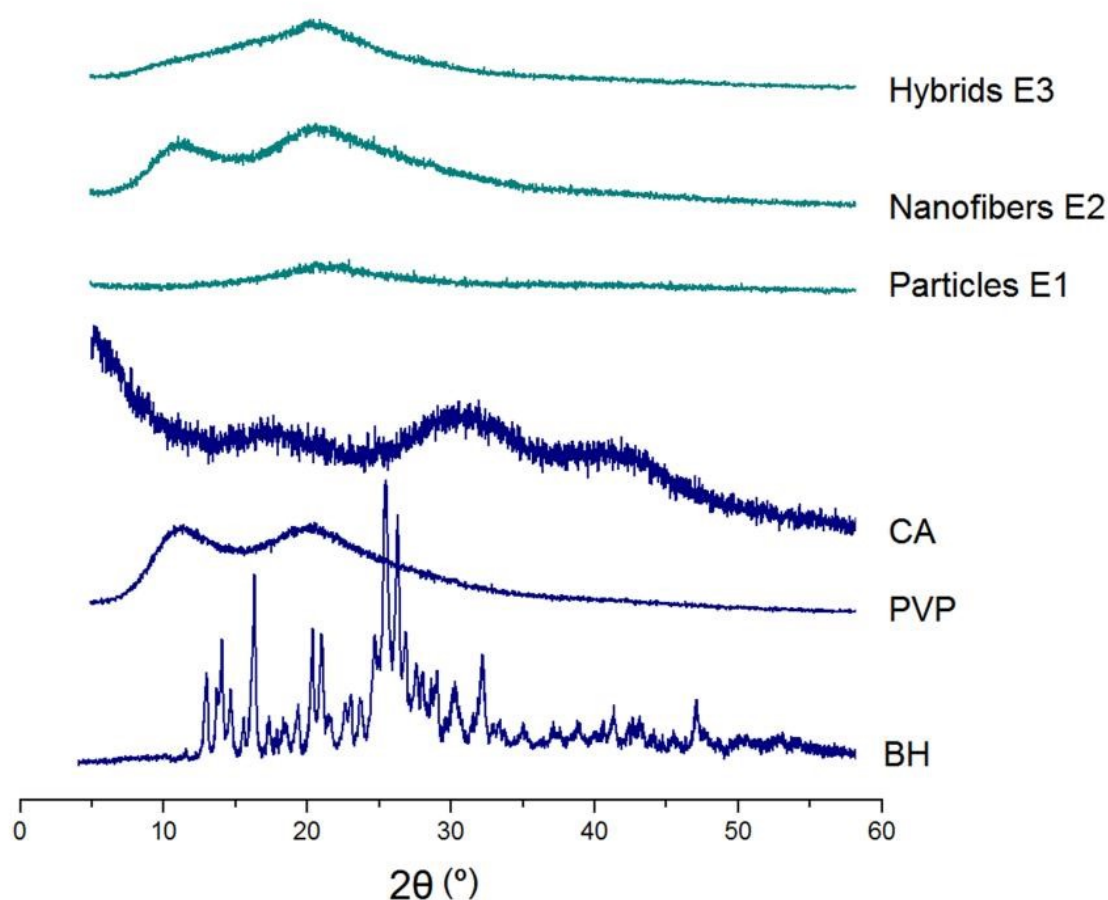


**Figure 6.** XRD patterns of the raw materials (CA, PVP, and BH) and their EHDAs products (hybrids E3, nanofibers E2, and particles E1).

FTIR spectra of the raw materials (CA, PVP, and BH) and their EHDAs products are shown in the left part of Figure 7. The molecular formats of CA, PVP, and BH are shown in the right part of Figure 7. CA had its characteristic peaks at 1724, 1376, 1236, and 1051  $\text{cm}^{-1}$ . PVP had its characteristic peaks at 1662, 1423, and 1291  $\text{cm}^{-1}$ . BH had the typical absorbance of 1740, 1598, and 1504  $\text{cm}^{-1}$ , owing to the three benzene rings in one BH molecule. Compared with the raw materials, the spectra of microparticles E1 were almost the same as CA with little hints from BH, suggesting E1 particles were composites. Similarly, the spectra of electrospun nanofibers E2 were similar to PVP, giving a hint that BH formed composites with PVP. In spectra of E1 and E2, the substantial decrease and even disappearance in the intensities of characteristic peaks and peaks in the finger regions of BH should be attributed to the secondary interactions between the drug BH and the polymeric carriers. These secondary interactions include hydrogen bonding, hydrophobic interactions, and electrostatic interactions, which favor the compatibility between the drug and its carrier and are beneficial to the stability of formed binary composites [77,78]. Compared with spectra of E1 and E2, the hybrids E3's spectra, on one hand, had also no BH sharp peaks and, thus, suggest an amorphous state of BH in them. On the other hand, E3's spectra was a superimposition of the spectra of E1 and E2 to a certain extent, suggesting that the ternary EHDAs products E3 were hybrids of the two binary composites.

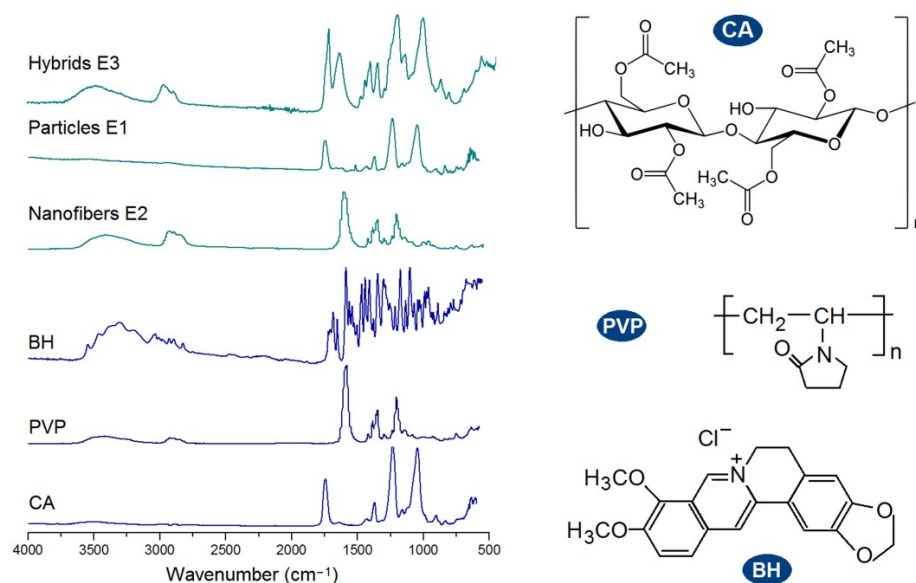


**Figure 7.** FTIR spectra of the raw materials (CA, PVP, and BH) and their EHDA products, and the molecular formats of the components within the EHDA products (CA, PVP, and BH).

### 3.4. In Vitro Drug Release Profiles

The pre-determined calibration equation for BH was  $A = 0.0688 \times C - 0.0047$  ( $R = 0.9999$ , and a linear range of 0.5 to 50  $\mu\text{g/mL}$ ), where  $A$  and  $C$  represent absorbance and BH concentration in  $\mu\text{g/mL}$ , respectively. The in vitro dissolution test results of the three types of EHDA products are shown in Figure 8. In Figure 8a,b, the curves were drawn according to the drug accumulative release percentage (%) vs. sampling time point (h), and in Figure 8c, the results are expressed according to the estimated durations vs. a certain percentage of BH (30%, 50%, and 90%).

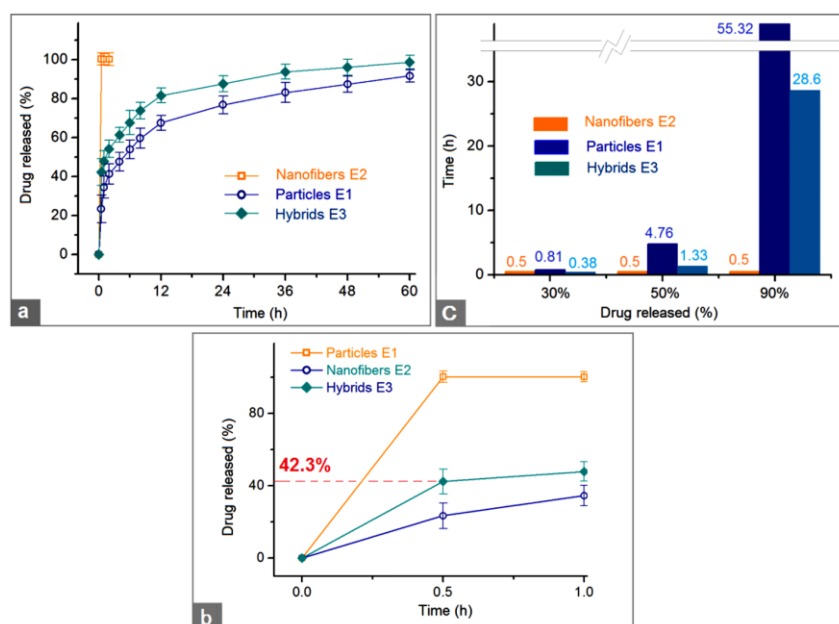


**Figure 8.** The in vitro dissolution test results: (a,b) drug accumulative release percentage (%) vs. sampling time point (h) for a whole experimental time and the first hour, respectively; and (c) estimated durations vs. a certain percentage of BH (30%, 50%, and 90%) that was released from the three EHDA products.

The first pre-determined time point for sampling was 0.5 h after the samples were placed into the dissolution media. The electrospun nanofibers E2 released all the loaded BH through an erosion mechanism, i.e., the drug BH and the polymeric matrix PVP were co-dissolved into the dissolution media (Figure 8b). This pulsatile release can be attributed to the following three reasons besides the fine solubility of PVP in water: (1) the small diameter of the nanofibers and the related large surface area, (2) the amorphous state of the drug BH, (3) the 3-D web structure of the fibrous mats and the related high porosity [79]. Compared with a 100% percentage release in 0.5 and 1 h, the electrospayed microparticles E2 and electrospun hybrids E3 released  $23.4 \pm 7.1\%$  and  $42.3 \pm 6.8\%$  after 0.5 h dissolution and  $34.5 \pm 5.6\%$  and  $47.9 \pm 5.3\%$  within one-hour dissolution, respectively. After a time period of 60 h dissolution, microparticles E2 and hybrids E3 released  $91.7 \pm 3.2\%$  and  $98.6 \pm 3.5\%$ , respectively. These data suggested that the hybrids E3 could provide a typical biphasic release profile with a release amount of 42.3% at the first phase in a pulsatile manner and 56.3% (98.6–42.3%) at the second phase in a sustained manner. It seems that the electrospayed particles E1 also furnished a biphasic release, i.e., 34.5% and 57.2% (91.7–34.5%) at the first and second phases, respectively. However, the release contents at different phases from hybrids E3 were intentionally tailored in a relatively accurate manner, whereas the release contents at different phases from the microparticles E1 were random and often uncontrollable. Thus, in pharmaceuticals, this case was regarded as an abnormal phenomenon to drug sustained release, i.e., initial burst effect.

The drug controlled release advantages of electrospun hybrids E3 over the electrospayed microparticles E1 can be further projected from Figure 8b. For a 30% release of the loaded BH, 0.38 h and 0.81 h were needed for the electrospun hybrids E3 and electrospayed microparticles E1, respectively. Meanwhile, for a 50% release of the loaded BH, 1.33 h and 4.76 h were needed for the electrospun hybrids E3 and electrospayed microparticles E1, respectively. For quickly reaching a therapeutic blood drug concentration, the faster the dosage forms can provide, the better effectiveness and compliance the patients have. From this standpoint, the hybrids E3 were apparently better than the microparticles E1.

For a 90% release of the loaded BH, 28.6 h and 55.32 h were needed for the electrospun hybrids E3 and electrospayed microparticles E1, respectively. In drug sustained release, an abnormal phenomenon is a tailing-off release, in which the drug is exhausted very slowly from its carrier and cannot keep an effective therapeutic blood drug concentration. The release percentage between 90% and 100% often falls within this abnormal region and should be avoided. From this standpoint, hybrids E3 are better than microparticle E1 due to a smaller tailing-off release and also a terminal release amount ( $98.7 \pm 3.5\%$  and  $91.8 \pm 3.2\%$  after 60 h for E3 and E1, respectively).

Additionally, the suspension fluid had an amount of 15.0 g microparticles E1 from electrospaying and 200 mL Fluid 2. The BH weight in the microparticles was  $15.0 \times 20\% = 3.0$  g. The BH weight in the nanofibers was  $4.0 \times (200 \text{ mL}/400 \text{ mL}) = 2.0$  g. Thus, in theory, the drug released in the first phase should be  $2.0/(2.0 + 3.0) \times 100\% = 40\%$ . The released BH from hybrids E3 after 0.5 and 1 h were  $42.3 \pm 6.8\%$  and  $47.9 \pm 5.3\%$ , respectively. The values were larger than the theoretically calculated value of 40%. This case should be attributed to both the preparation of working suspensions for creating hybrids E3 and drug release from the particles. Some surface BH on the surface of electrospayed microparticles E1 should re-dissolve into the suspensions, making a little higher drug concentration in the hydrophilic PVP. Further studies may be designed to improve the accuracy of drug release contents at different phases, e.g., a blank CA coating on the microparticles through coaxial electrospaying.

### 3.5. Drug Release Mechanism

To disclose the drug release mechanism, the Peppas equation ( $Q = kt^n$ , where  $Q$  is the drug release content,  $k$  is a constant, and  $t$  is an indicator of drug release behaviors [80]) was exploited to regress the BH release data achieved during the in vitro dissolution tests (time  $\geq 1$  h). The results for the electrospayed microparticles E1 and

electrospun hybrids E3 are exhibited in Figure 9. For particles E1, the regressed equation was  $\text{Log}Q = 1.54 + 0.24 \text{Log}t$  ( $R = 0.9968$ ). For the second phase of hybrids E3, the regressed equation was  $\text{Log}Q = 1.69 + 0.18 \text{Log}t$  ( $R = 0.9924$ ). Both EHDA products had an  $n$  value smaller than the critical judgment value of 0.45, suggesting that BH was released from the CA microparticles through a typical Fickian diffusion mechanism, regardless of a sole state of microparticles E1 or a co-existing state with hydrophilic polymer PVP in hybrids E3.

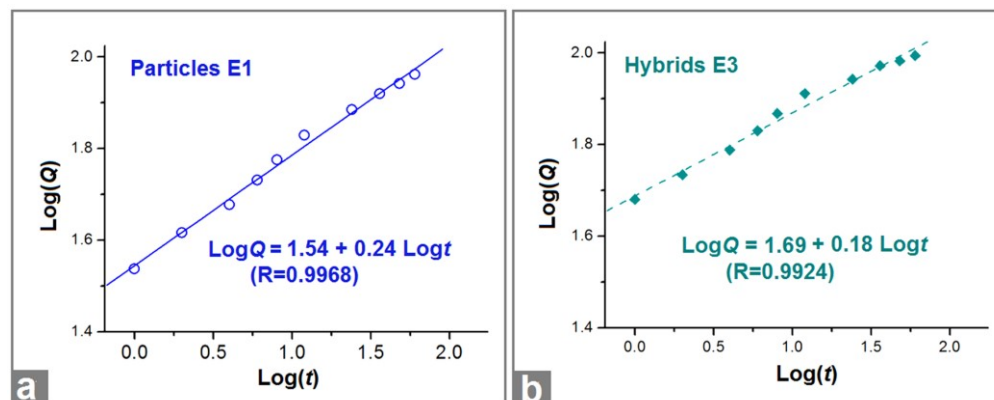


**Figure 9.** The regressed equations drawn from the in vitro BH release data of particles E1 (a) and hybrids E3 (b).

After a full time period of 60 h dissolution, the residue particles were taken out from the in vitro dissolution vessels and naturally dried. These particles experienced SEM evaluations. Their images are exhibited in Figure 10. Compared with the previous images before dissolution, both microparticles E1 (Figure 10a) particles in hybrids E3 (Figure 10b) lost their original smooth surface and solid state, but they exhibited a porous surface and a more concave morphology. Apparently, those surface holes and deformed surface morphology (resulted from a void inner) were direct outcomes owing to the removal of loaded BH molecules, providing an intuitive clue of a drug diffusion mechanism from the insoluble CA matrix. Compared with previous reports of biphasic release from electrospun core-sheath nanofibers [81], hybrids of electrospun nanofibers and casting films [82], and electrospun Janus nanofibers [83], the present trans-scale hybrids E3 showed a longer sustained release second phase and a better biphasic release profile.

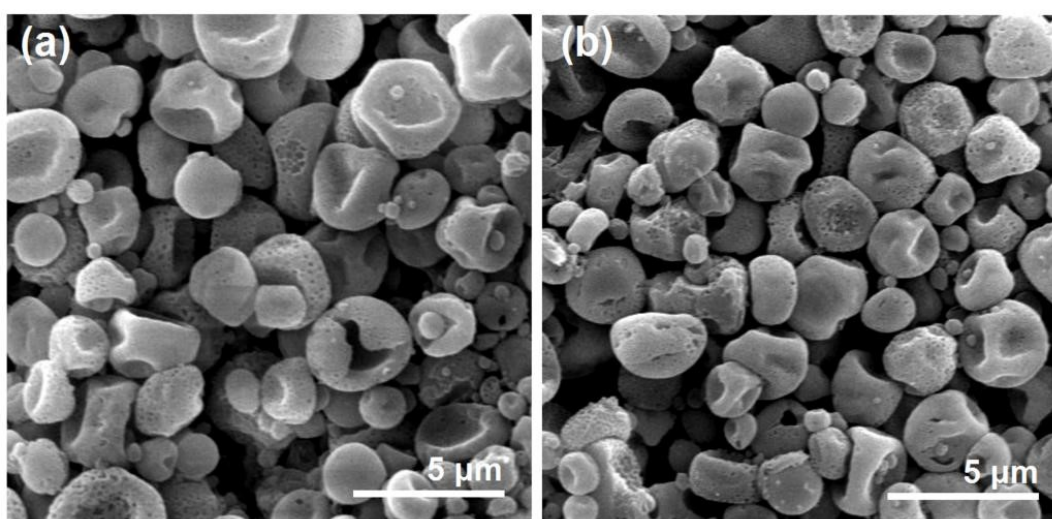


**Figure 10.** The SEM images of the residue microparticles after the exhaustion of BH molecules from the microparticles E1 (a) and the hybrids E3 (b).

Based on the above-mentioned analyses, a diagram is shown in Figure 11. The combined mechanism of the BH biphasic release from the hybrids E3 containing electrospun PVP nanofibers and electrospayed CA microparticles was clear. When the hybrids E3 are placed into the dissolution media, the BH-PVP nanofibers will be rapidly dissolved. This is a typical erosion process for the fast release of BH in the first phase. Later, the BH molecules distributed or absorbed on the surface of CA microparticles would dissolve into the dissolution media, by which the routes for water molecules' penetration into the inner sections of CA particles gradually open. Along with the penetration of water molecules from surface to the core of CA microparticles, the loaded drug BH molecules would be free and inversely diffused from the CA particles to the bulk solution. During all the processes, the CA skeleton is insoluble and keeps the routes for diffusions and exchanges of both water and BH molecules. In theory, the diffusion process will not be terminated until a uniform BH distribution all over the bulk solution and a dynamic absorbance balance between the dissolution media and solid CA skeleton. After the CA skeletons are fetched out and dried, it is inevitable for them to experience some deformations.

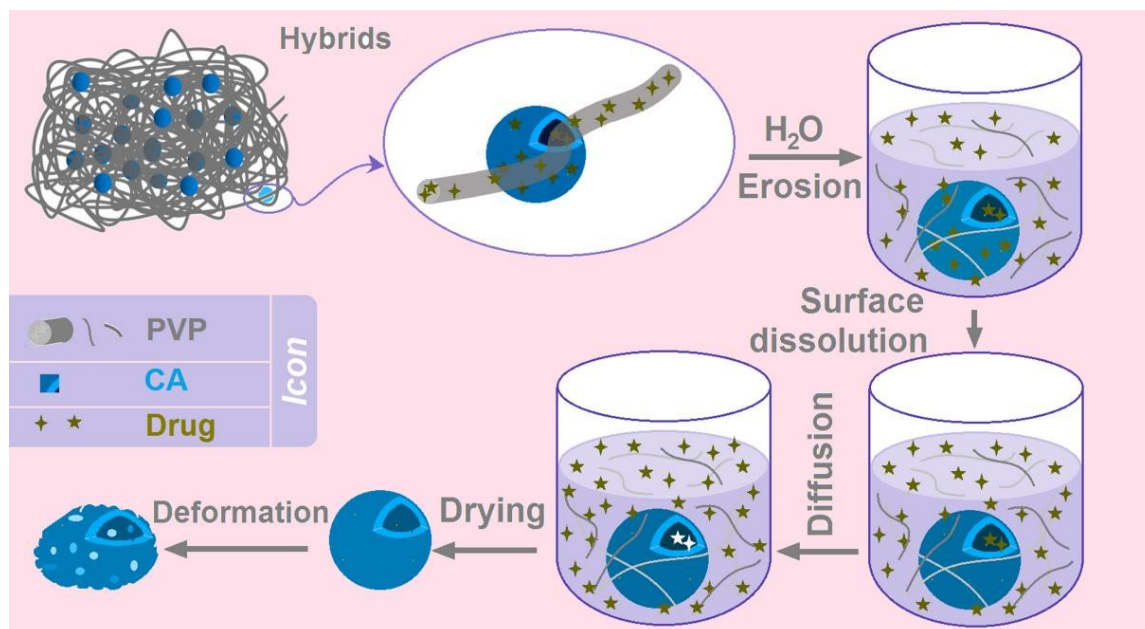


**Figure 11.** The mechanism about the biphasic release of BH from the hybrids of electrospun PVP nanofibers and electrospayed CA microparticles.

New methods for human health are always highly desired [84–89]. Today, on one hand, numerous strategies were reported in the literature to create novel functional ingredients on a molecular scale with chemical reactions as the fundamental supports [90–95]. On the other hand, new methods bloomed in manipulating the molecules into nano aggregates from both “top-down” manner and “bottom-up” way [96–101]. In this study, a new concept was demonstrated and a trans-dimensional strategy was explored to generate functional hybrid materials through a combination of nanoproductions and products at microscale for an improved final functional performance. Based on the protocols reported here, there are a wide variety of possibilities for conceiving novel functional materials in the future.

#### 4. Conclusions

In this study, a sequential EHDA process was successfully developed for creating a new kind of medicated hybrids E3. The hybrids E3 contained both BH-loaded hydrophilic PVP nanofibers and insoluble BH-loaded CA microparticles. The key element was that the electrospayed BH-CA microparticles were insoluble in the solvent mixture of DCM and DMAc (with a volume ratio of 9:1) and, thus, an electrospinnable suspension was

prepared, and in turn, the nanofiber-microparticle hybrids E3 were achieved through the single-fluid electrospinning process. The routine characterization results indicated that the hybrids E3 were a mixture of particles and nanofibers with BH distributed in the PVP and CA matrices in an amorphous state. In vitro dissolution tests demonstrated that the hybrids E3 were able to furnish the designed biphasic release profile, with a 42.3% drug release at the first immediate release phase and a 56.3% drug release at the second phase in a sustained manner. The BH molecule release was manipulated through a combination of molecular erosion mechanism and the typical molecular Fickian diffusion mechanism. This research paves a new way for developing functional materials through organizing materials at different scale levels and with different outer shapes.

**Author Contributions:** Conceptualization, J.Z. and Y.D.; methodology, J.Z., Y.D., J.F. and C.Y.; writing—original draft preparation, J.Z. and D.-G.Y.; writing—review and editing, D.-G.Y. and T.Y.; visualization, J.F. and C.Y.; supervision, D.-G.Y.; project administration, D.-G.Y.; funding acquisition, D.-G.Y. and T.Y. All authors have read and agreed to the published version of the manuscript.

**Funding:** This investigation was financially supported by the Shanghai Natural Science Foundation (No. 20ZR1439000), the Macao Polytechnic University Research Fund (RP/FCSD-01/2023), and the Innovation Projects for USST students to J.F. and C.Y. (Nos. SH2022225 and SH2022229).

**Institutional Review Board Statement:** Not applicable.

**Informed Consent Statement:** Not applicable.

**Data Availability Statement:** The data supporting the findings of this manuscript are available from the corresponding authors upon reasonable.

**Acknowledgments:** Wanli He is appreciated for his support.

**Conflicts of Interest:** The authors declare no conflict of interest.

## References

1. Chen, G.; Kong, P.; Jiang, A.; Wang, X.; Sun, Y.; Yu, T.; Chi, H.; Song, C.; Zhang, H.; Subedi, D.; et al. A Modular Programmed Biphasic Dual-Delivery System on 3D Ceramic Scaffolds for Osteogenesis in Vitro and in Vivo. *J. Mater. Chem. B* **2020**, *8*, 9697–9717. [[CrossRef](#)]
2. Ejeta, F.; Gabriel, T.; Joseph, N.M.; Belete, A. Formulation, Optimization and In Vitro Evaluation of Fast Disintegrating Tablets of Salbutamol Sulphate Using a Combination of Superdisintegrant and Subliming Agent. *Curr. Drug Deliv.* **2022**, *19*, 129–141.
3. Kose, M.D.; Ungun, N.; Bayraktar, O. Eggshell Membrane Based Turmeric Extract Loaded Orally Disintegrating Films. *Curr. Drug Deliv.* **2022**, *19*, 547–559. [[PubMed](#)]
4. Phaechemud, T.; Choncheewa, C. Double-Layered Matrix of Shellac Wax-Lutrol in Controlled Dual Drug Release. *AAPS PharmSciTech* **2016**, *17*, 1326–1335. [[CrossRef](#)]
5. Beugeling, M.; Grasmeijer, N.; Born, P.A.; van der Meulen, M.; van der Kooij, R.S.; Schwengle, K.; Baert, L.; Amssoms, K.; Frijlink, H.W.; Hinrichs, W.L.J. The Mechanism behind the Biphasic Pulsatile Drug Release from Physically Mixed Poly(DL-Lactic(-Co-Glycolic) Acid)-Based Compacts. *Int. J. Pharm.* **2018**, *551*, 195–202. [[CrossRef](#)] [[PubMed](#)]
6. Zhou, J.; Wang, P.; Yu, D.G.; Zhu, Y. Biphasic Drug Release from Electrospun Structures. *Expert Opin. Drug Deliv.* **2023**, *20*, 621–640. [[CrossRef](#)]
7. Chen, Y.; Yu, W.; Qian, X.; Li, X.; Wang, Y.; Ji, J. Dissolving Microneedles with a Biphasic Release of Antibacterial Agent and Growth Factor to Promote Wound Healing. *Biomater. Sci.* **2022**, *10*, 2409–2416. [[CrossRef](#)]
8. Tung, N.-T.; Dong, T.-H.-Y.; Tran, C.-S.; Nguyen, T.-K.-T.; Chi, S.-C.; Dao, D.-S.; Nguyen, D.-H. Integration of Lornoxicam Nanocrystals into Hydroxypropyl Methylcellulose-Based Sustained Release Matrix to Form a Novel Biphasic Release System. *Int. J. Biol. Macromol.* **2022**, *209*, 441–451. [[CrossRef](#)] [[PubMed](#)]
9. Adala, I.; Ramis, J.; Moussinga, C.N.; Janowski, I.; Amer, M.H.; Bennett, A.J.; Alexander, C.; Rose, F.R.A.J. Mixed Polymer and Bioconjugate Core/Shell Electrospun Fibres for Biphasic Protein Release. *J. Mater. Chem. B* **2021**, *9*, 4120–4133. [[CrossRef](#)] [[PubMed](#)]
10. Conceicao, J.; Adeoye, O.; Cabral-Marques, H.; Concheiro, A.; Alvarez-Lorenzo, C.; Sousa Lobo, J.M. Carbamazepine Bilayer Tablets Combining Hydrophilic and Hydrophobic Cyclodextrins as a Quick/Slow Biphasic Release System. *J. Drug Deliv. Sci. Technol.* **2020**, *57*, 101611. [[CrossRef](#)]
11. Yang, B.; Dong, Y.; Shen, Y.; Hou, A.; Quan, G.; Pan, X.; Wu, C. Bilayer Dissolving Microneedle Array Containing 5-Fluorouracil and Triamcinolone with Biphasic Release Profile for Hypertrophic Scar Therapy. *Bioact. Mater.* **2021**, *6*, 2400–2411. [[CrossRef](#)]
12. He, H.; Wu, M.; Zhu, J.W.; Yang, Y.Y.; Ge, R.L.; Yu, D.G. Engineered Spindles of Little Molecules Around Electrospun Nanofibers for Biphasic Drug Release. *Adv. Fiber Mater.* **2022**, *4*, 305–317. [[CrossRef](#)]

13. Tabakoglu, S.; Kolbuk, D.; Sajkiewicz, P. Multifluid Electrospinning for Multi-Drug Delivery Systems: Pros and Cons, Challenges, and Future Directions. *Biomater. Sci.* **2022**, *11*, 37–61. [[CrossRef](#)]
14. Hameed, A.; Rehman, T.U.; Rehan, Z.A.; Noreen, R.; Iqbal, S.; Batool, S.; Qayyum, M.A.; Ahmed, T.; Farooq, T. Development of Polymeric Nanofibers Blended with Extract of Neem (*Azadirachta indica*), for Potential Biomedical Applications. *Front. Mater.* **2022**, *9*, 1042304. [[CrossRef](#)]
15. Brimo, N.; Serdaroglu, D.C.; Uysal, B. Comparing Antibiotic Pastes with Electrospun Nanofibers as Modern Drug Delivery Systems for Regenerative Endodontics. *Curr. Drug Deliv.* **2022**, *19*, 904–917.
16. Kuang, G.; Zhang, Z.; Liu, S.; Zhou, D.; Lu, X.; Jing, X.; Huang, Y. Biphasic Drug Release from Electrospun Polyblend Nanofibers for Optimized Local Cancer Treatment. *Biomater. Sci.* **2018**, *6*, 324–331. [[CrossRef](#)]
17. Yang, S.; Li, X.; Liu, P.; Zhang, M.; Wang, C.; Zhang, B. Multifunctional Chitosan/Polycaprolactone Nanofiber Scaffolds with Varied Dual-Drug Release for Wound-Healing Applications. *ACS Biomater. Sci. Eng.* **2020**, *6*, 4666–4676. [[CrossRef](#)] [[PubMed](#)]
18. Lee, H.; Xu, G.; Kharaghani, D.; Nishino, M.; Song, K.H.; Lee, J.S.; Kim, I.S. Electrospun Tri-Layered Zein/PVP-GO/Zein Nanofiber Mats for Providing Biphasic Drug Release Profiles. *Int. J. Pharm.* **2017**, *531*, 101–107. [[CrossRef](#)] [[PubMed](#)]
19. Khalek, M.A.A.; Gaber, S.A.A.; El-Domany, R.A.; El-Kemary, M.A. Photoactive Electrospun Cellulose Acetate/Polyethylene Oxide/Methylene Blue and Trilayered Cellulose Acetate/Polyethylene Oxide/Silk Fibroin/Ciprofloxacin Nanofibers for Chronic Wound Healing. *Int. J. Biol. Macromol.* **2021**, *193*, 1752–1766. [[CrossRef](#)]
20. Zhou, H.Y.; Tong, J.N.; Ren, L.J.; Hao, P.Y.; Zheng, H.J.; Guo, X.M.; Chen, Y.W.; Li, J.B.; Park, H.J. Preparation and Performance of Chitosan/Cyclodextrin-g-Glutamic Acid Thermosensitive Hydrogel. *J. Drug Deliv. Sci. Technol.* **2022**, *74*, 103504. [[CrossRef](#)]
21. Peng, L.; Kang, S.; Yin, Z.; Jia, R.; Song, X.; Li, L.; Li, Z.; Zou, Y.; Liang, X.; Li, L.; et al. Antibacterial Activity and Mechanism of Berberine against *Streptococcus Agalactiae*. *Int. J. Clin. Exp. Pathol.* **2015**, *8*, 5217–5223.
22. Roy, R.; Tiwari, M.; Donelli, G.; Tiwari, V. Strategies for Combating Bacterial Biofilms: A Focus on Anti-Biofilm Agents and Their Mechanisms of Action. *Virulence* **2018**, *9*, 522–554. [[CrossRef](#)]
23. Tan, X.-S.; Ma, J.-Y.; Feng, R.; Ma, C.; Chen, W.-J.; Sun, Y.-P.; Fu, J.; Huang, M.; He, C.-Y.; Shou, J.-W.; et al. Tissue Distribution of Berberine and Its Metabolites after Oral Administration in Rats. *PLoS ONE* **2013**, *8*, e77969. [[CrossRef](#)]
24. Wang, X.; Feng, C. Chiral Fiber Supramolecular Hydrogels for Tissue Engineering. *Wiley Interdiscip. Rev. Nanomed. Nanobiotechnol.* **2023**, *15*, e1847. [[CrossRef](#)]
25. Esquivel, S.V.; Bhatt, H.N.; Diwan, R.; Habib, A.; Lee, W.-Y.; Khatun, Z.; Nurunnabi, M.  $\beta$ -Glucan and Fatty Acid Based Mucoadhesive Carrier for Gastrointestinal Tract Specific Local and Sustained Drug Delivery. *Biomolecules* **2023**, *13*, 768. [[CrossRef](#)]
26. Yu, D.-G.; Zhao, P. The Key Elements for Biomolecules to Biomaterials and to Bioapplications. *Biomolecules* **2022**, *12*, 1234. [[CrossRef](#)] [[PubMed](#)]
27. Kramar, A.; González-Benito, J. Preparation of Cellulose Acetate Film with Dual Hydrophobic-Hydrophilic Properties Using Solution Blow Spinning. *Mater. Des.* **2023**, *227*, 111788. [[CrossRef](#)]
28. Song, W.; Zhang, Y.; Tran, C.H.; Choi, H.K.; Yu, D.G.; Kim, I. Porous Organic Polymers with Defined Morphologies: Synthesis, Assembly, and Emerging Applications. *Prog. Polym. Sci.* **2023**, *142*, 101691. [[CrossRef](#)]
29. Huang, J.; Feng, C. Aniline Dimers Serving as Stable and Efficient Transfer Units for Intermolecular Charge-Carrier Transmission. *iScience* **2023**, *26*, 105762. [[CrossRef](#)]
30. Zhang, Y.; Liu, X.; Geng, C.; Shen, H.; Zhang, Q.; Miao, Y.; Wu, J.; Ouyang, R.; Zhou, S. Two Hawks with One Arrow: A Review on Bifunctional Scaffolds for Photothermal Therapy and Bone Regeneration. *Nanomaterials* **2023**, *13*, 551. [[CrossRef](#)]
31. Qi, Q.; Wang, Q.; Li, Y.; Silva, D.Z.; Ruiz, M.E.L.; Ouyang, R.; Liu, B.; Miao, Y. Recent Development of Rhenium-Based Materials in the Application of Diagnosis and Tumor Therapy. *Molecules* **2023**, *28*, 2733. [[CrossRef](#)]
32. Wang, L.; Ahmad, Z.; Huang, J.; Li, J.-S.; Chang, M.-W. Multi-Compartment Centrifugal Electrospinning Based Composite Fibers. *Chem. Eng. J.* **2017**, *330*, 541–549. [[CrossRef](#)]
33. Sivan, M.; Madheswaran, D.; Hauzerova, S.; Novotny, V.; Hedvicakova, V.; Jencova, V.; Kostakova, E.K.; Schindler, M.; Lukas, D. AC Electrospinning: Impact of High Voltage and Solvent on the Electrospinnability and Productivity of Polycaprolactone Electrospun Nanofibrous Scaffolds. *Mater. Today Chem.* **2022**, *26*, 101025. [[CrossRef](#)]
34. Zhou, Y.; Wang, M.; Yan, C.; Liu, H.; Yu, D.-G. Advances in the Application of Electrospun Drug-Loaded Nanofibers in the Treatment of Oral Ulcers. *Biomolecules* **2022**, *12*, 1254. [[CrossRef](#)] [[PubMed](#)]
35. Wang, X.; Peng, Y.; Wu, Y.; Cao, S.; Deng, H.; Cao, Z. Chitosan/Silk Fibroin Composite Bilayer PCL Nanofibrous Mats for Bone Regeneration with Enhanced Antibacterial Properties and Improved Osteogenic Potential. *Int. J. Biolog. Macromol.* **2023**, *230*, 123265. [[CrossRef](#)] [[PubMed](#)]
36. Wang, Q.; Liu, Q.; Gao, J.; He, J.; Zhang, H.; Ding, J. Stereo Coverage and Overall Stiffness of Biomaterial Arrays Underly Parts of Topography Effects on Cell Adhesion. *ACS Appl. Mater. Interfaces* **2023**, *15*, 6142–6155. [[CrossRef](#)] [[PubMed](#)]
37. Chen, W.; Zhao, P.; Yang, Y.; Yu, D. Electrospun Beads-on-the-String Nanoproducts: Preparation and Drug Delivery Application. *Curr. Drug Deliv.* **2022**, *19*, 1224–1240.
38. Huang, H.; Song, Y.; Zhang, Y.; Li, Y.; Li, J.; Lu, X.; Wang, C. Electrospun Nanofibers: Current Progress and Applications in Food Systems. *J. Agric. Food Chem.* **2022**, *70*, 1391–1409. [[CrossRef](#)]
39. Wang, Y.; Yu, D.-G.; Liu, Y.; Liu, Y.-N. Progress of Electrospun Nanofibrous Carriers for Modifications to Drug Release Profiles. *J. Func. Biomater.* **2022**, *13*, 289. [[CrossRef](#)]

40. Shen, S.-F.; Zhu, L.-F.; Liu, J.; Ali, A.; Zaman, A.; Ahmad, Z.; Chen, X.; Chang, M.-W. Novel Core-Shell Fiber Delivery System for Synergistic Treatment of Cervical Cancer. *J. Drug Del. Sci. Technol.* **2020**, *59*, 101865. [[CrossRef](#)]
41. Yildiz, Z.I.; Topuz, F.; Kilic, M.E.; Durgun, E.; Uyar, T. Encapsulation of Antioxidant Beta-carotene by Cyclodextrin Complex Electrospun Nanofibers: Solubilization and Stabilization of Beta-Carotene by Cyclodextrins. *Food Chem.* **2023**, *423*, 136284. [[CrossRef](#)]
42. Guler, E.; Nur Hazar-Yavuz, A.; Tatar, E.; Morid Haidari, M.; Sinemcan Ozcan, G.; Duruksu, G.; Graça, M.P.F.; Kalaskar, D.M.; Gunduz, O.; Emin Cam, M. Oral Empagliflozin-Loaded Tri-Layer Core-Sheath Fibers Fabricated Using Tri-Axial Electrospinning: Enhanced in Vitro and in Vivo Antidiabetic Performance. *Int. J. Pharm.* **2023**, *635*, 122716. [[CrossRef](#)]
43. Afshar, S.K.; Abdorashidi, M.; Dorkoosh, F.A.; Akbari Javar, H. Electrospun Fibers: Versatile Approaches for Controlled Release Applications. *Int. J. Polym. Sci.* **2022**, *2022*, 9116168.
44. Shen, Y.; Yu, X.; Cui, J.; Yu, F.; Liu, M.; Chen, Y.; Wu, J.; Sun, B.; Mo, X. Development of Biodegradable Polymeric Stents for the Treatment of Cardiovascular Diseases. *Biomolecules* **2022**, *12*, 1245. [[CrossRef](#)]
45. Wang, M.; Ge, R.; Zhao, P.; Williams, G.R.; Yu, D.-G.; Bligh, S.W.A. Exploring Wettability Difference-Driven Wetting by Utilizing Electrospun Chimeric Janus Microfiber Comprising Cellulose Acetate and Polyvinylpyrrolidone. *Mater. Design* **2023**, *226*, 111652. [[CrossRef](#)]
46. Wang, M.; Ge, R.L.; Zhang, F.; Yu, D.G.; Liu, Z.P.; Li, X.; Shen, H.; Williams, G.R. Electrospun fibers with blank surface and inner drug gradient for improving sustained release. *Biomater. Adv.* **2023**, *150*, 213404. [[CrossRef](#)]
47. Yao, Z.-C.; Zhang, C.; Ahmad, Z.; Huang, J.; Li, J.-S.; Chang, M.-W. Designer Fibers from 2D to 3D-Simultaneous and Controlled Engineering of Morphology, Shape and Size. *Chem. Eng. J.* **2018**, *334*, 89–98. [[CrossRef](#)]
48. Lv, H.; Liu, Y.; Bai, Y.; Shi, H.; Zhou, W.; Chen, Y.; Liu, Y.; Yu, D.-G. Recent Combinations of Electrospinning with Photocatalytic technology for Treating Polluted Water. *Catalysts* **2023**, *13*, 758. [[CrossRef](#)]
49. Feng, Z.; Zhao, Z.; Liu, Y.; Liu, Y.; Cao, X.; Yu, D.G.; Wang, K. Piezoelectric Effect Polyvinylidene Fluoride (PVDF): From Energy Harvester to Smart Skin and Electronic Textiles. *Adv. Mater. Technol.* **2023**. [[CrossRef](#)]
50. Wang, P.; Lv, H.; Cao, X.; Liu, Y.; Yu, D.-G. Recent Progress of the Preparation and Application of Electrospun Porous Nanofibers. *Polymers* **2023**, *15*, 921. [[CrossRef](#)] [[PubMed](#)]
51. Yu, D.G.; Yu, J.; Chen, L.; Williams, G.R.; Wang, X. Modified Coaxial Electrospinning for the Preparation of High-Quality Ketoprofen-Loaded Cellulose Acetate Nanofibers. *Carbohydr. Polym.* **2012**, *90*, 1016–1023. [[CrossRef](#)]
52. Du, Y.; Yu, D.-G.; Yi, T. Electrospun Nanofibers as Chemosensors for Detecting Environmental Pollutants: A Review. *Chemosensors* **2023**, *11*, 208. [[CrossRef](#)]
53. Wang, X.; Qi, Y.; Hu, Z.; Jiang, L.; Pan, F.; Xiang, Z.; Xiong, Z.; Jia, W.; Hu, J.; Lu, W. Fe<sub>3</sub>O<sub>4</sub>@PVP@DOX Magnetic Vortex Hybrid Nanostructures with Magnetic-Responsive Heating and Controlled Drug Delivery Functions for Precise Medicine of Cancers. *Adv. Compos. Hybrid. Mater.* **2022**, *5*, 1786–1798. [[CrossRef](#)]
54. Liu, H.; Bai, Y.; Huang, C.; Wang, Y.; Ji, Y.; Du, Y.; Xu, L.; Yu, D.-G.; Bligh, S.W.A. Recent Progress of Electrospun Herbal Medicine Nanofibers. *Biomolecules* **2023**, *13*, 184. [[CrossRef](#)]
55. Wang, M.-L.; Yu, D.-G.; Bligh, S.W.A. Progress in Preparing Electrospun Janus Fibers and Their Applications. *Appl. Mater. Today* **2023**, *31*, 101766. [[CrossRef](#)]
56. Yao, L.; Sun, C.; Lin, H.; Li, G.; Lian, Z.; Song, R.; Zhuang, S.; Zhang, D. Electrospun Bi-Decorated BiTiO<sub>2</sub>/TiO<sub>2</sub> Flexible Carbon Nanofibers and Their Applications on Degrading of Organic Pollutants under Solar Radiation. *J. Mater. Sci. Technol.* **2023**, *150*, 114–123. [[CrossRef](#)]
57. Yao, Z.-C.; Yuan, Q.; Ahmad, Z.; Huang, J.; Li, J.-S.; Chang, M.-W. Controlled Morphing of Microbubbles to Beaded Nanofibers via Electrically Forced Thin Film Stretching. *Polymers* **2017**, *9*, 265. [[CrossRef](#)]
58. Song, W.; Tang, Y.; Qian, C.; Kim, B.J.; Liao, Y.; Yu, D.-G. Electrospinning Spinneret: A Bridge between the Visible World and the Invisible Nanostructures. *Innovation* **2023**, *4*, 100381. [[CrossRef](#)]
59. Yao, L.; Sun, C.; Lin, H.; Li, G.; Lian, Z.; Song, R.; Zhuang, S.; Zhang, D. Enhancement of AFB1 Removal Efficiency via Adsorption/Photocatalysis Synergy Using Surface-Modified Electrospun PCL-g-C<sub>3</sub>N<sub>4</sub>/CQDs Membranes. *Biomolecules* **2023**, *13*, 550. [[CrossRef](#)]
60. Li, H.; Zhang, Z.; Ren, Z.; Chen, Y.; Huang, J.; Lei, Z.; Qian, X.; Lai, Y.; Zhang, S. A Quadruple Biomimetic Hydrophilic/Hydrophobic Janus Composite Material Integrating Cu(OH)<sub>2</sub> Micro-Needles and Embedded Bead-on-String Nanofiber Membrane for Efficient Fog Harvesting. *Chem. Eng. J.* **2023**, *455*, 140863. [[CrossRef](#)]
61. Yu, D.G.; Xu, L. Impact Evaluations of Articles in Current Drug Delivery Based on Web of Science. *Curr. Drug Deliv.* **2023**, *20*. [[CrossRef](#)] [[PubMed](#)]
62. Xu, J.; Zhong, M.; Song, N.; Wang, C.; Lu, X. General Synthesis of Pt and Ni Co-Doped Porous Carbon Nanofibers to Boost HER Performance in Both Acidic and Alkaline Solutions. *Chin. Chem. Lett.* **2023**, *34*, 107359. [[CrossRef](#)]
63. Yang, Y.; Chen, W.; Wang, M.; Shen, J.; Tang, Z.; Qin, Y.; Yu, D.-G. Engineered Shellac Beads-On-The-String Fibers Using Triaxial Electrospinning for Improved Colon-Targeted Drug Delivery. *Polymers* **2023**, *15*, 2237. [[CrossRef](#)]
64. Lv, H.; Liu, Y.; Zhao, P.; Bai, Y.; Cui, W.; Shen, S.; Liu, Y.; Wang, Z.; Yu, D.-G. Insight into the Superior Piezophotocatalytic Performance of BaTiO<sub>3</sub>/ZnO Janus Nanofibrous Heterostructures in the Treatment of Multi-Pollutants from Water. *Appl. Catal. B Environ.* **2023**, *330*, 122623. [[CrossRef](#)]



65. Cao, X.; Chen, W.; Zhao, P.; Yang, Y.; Yu, D.-G. Electrospun Porous Nanofibers: Pore-Forming Mechanisms and Applications for Photocatalytic Degradation of Organic Pollutants in Wastewater. *Polymers* **2022**, *14*, 3990. [[CrossRef](#)]
66. Bai, Y.; Liu, Y.; Lv, H.; Shi, H.; Zhou, W.; Liu, Y.; Yu, D.-G. Processes of Electrospun Polyvinylidene Fluoride-Based Nanofibers, Their Piezoelectric Properties, and Several Fantastic Applications. *Polymers* **2022**, *14*, 4311. [[CrossRef](#)] [[PubMed](#)]
67. Zhu, M.; Yu, J.; Li, Z.; Ding, B. Self-Healing Fibrous Membranes. *Angew. Chem.-Int. Edit.* **2022**, *61*, e202208949. [[CrossRef](#)]
68. Guastaferrero, M.; Baldino, L.; Cardea, S.; Reverchon, E. Supercritical assisted electrospray/spinning to produce PVP+quercetin microparticles and microfibers. *J. Taiwan Inst. Chem. Eng.* **2020**, *117*, 278–286. [[CrossRef](#)]
69. Chen, R.; Shi, J.; Liu, C.; Li, J.; Cao, S. In Situ Self-Assembly of Gold Nanorods with Thermal-Responsive Microgel for Multi-Synergistic Remote Drug Delivery. *Adv. Compos. Hybrid. Mater.* **2022**, *5*, 2223–2234. [[CrossRef](#)]
70. Wang, Z.; Li, R.; Zhang, J. On-Demand Drug Delivery of Triptolide and Celastrol by Poly(Lactic-Co-Glycolic Acid) Nanoparticle/Triglycerol Monostearate-18 Hydrogel Composite for Rheumatoid Arthritis Treatment. *Adv. Compos. Hybrid. Mater.* **2022**, *5*, 2921–2935. [[CrossRef](#)]
71. Yao, Z.-C.; Gao, Y.; Chang, M.-W.; Ahmad, Z.; Li, J.-S. Regulating Polycaprolactone Fiber Characteristics In-Situ During One-Step Coaxial Electrospinning via Enveloping Liquids. *Mater. Lett.* **2016**, *183*, 202–206. [[CrossRef](#)]
72. Yu, D.-G.; Du, Y.; Chen, J.; Song, W.; Zhou, T. A Correlation Analysis between Undergraduate Students' Safety Behaviors in the Laboratory and Their Learning Efficiencies. *Behav. Sci.* **2023**, *13*, 127. [[CrossRef](#)]
73. Kang, S.; Hou, S.; Chen, X.; Yu, D.-G.; Wang, L.; Li, X.; Williams, R.G. Energy-Saving Electrospinning with a Concentric Teflon-Core Rod Spinneret to Create Medicated Nanofibers. *Polymers* **2020**, *12*, 2421. [[CrossRef](#)] [[PubMed](#)]
74. Han, W.; Wang, L.; Li, Q.; Ma, B.; He, C.; Guo, X.; Nie, J.; Ma, G. A Review: Current Status and Emerging Developments on Natural Polymer-Based Electrospun Fibers. *Macromol. Rapid Commun.* **2022**, *43*, 2200456. [[CrossRef](#)]
75. Wang, H.; Lu, H.; Yang, H.; Yu, D.G.; Lu, H. The Influence of the Ultrasonic Treatment of Working Fluids on Electrospun Amorphous Solid Dispersions. *Front. Mol. Biosci.* **2023**, *10*, 1184767. [[CrossRef](#)]
76. Wang, M.; Hou, J.; Yu, D.-G.; Li, S.; Zhu, J.; Chen, Z. Electrospun Tri-Layer Nanodepots for Sustained Release of Acyclovir. *J. Alloys Compd.* **2020**, *846*, 156471. [[CrossRef](#)]
77. Huang, X.; Jiang, W.; Zhou, J.; Yu, D.-G.; Liu, H. The Applications of Ferulic-Acid-Loaded Fibrous Films for Fruit Preservation. *Polymers* **2022**, *14*, 4947. [[CrossRef](#)]
78. Jiang, W.; Zhang, X.; Liu, P.; Zhang, Y.; Song, W.; Yu, D.-G.; Lu, X. Electrospun Healthcare Nanofibers from Medicinal Liquor of *Phellinus igniarius*. *Adv. Compos. Hybrid Mater.* **2022**, *5*, 3045–3056. [[CrossRef](#)]
79. Yu, D.G.; Li, J.; Williams, G.R.; Zhao, M. Electrospun amorphous solid dispersions of poorly water-soluble drugs: A review. *J. Control. Release* **2018**, *292*, 91–110. [[CrossRef](#)] [[PubMed](#)]
80. Peppas, N.A. Analysis of Fickian and Non-Fickian Drug Release from Polymers. *Pharm. Acta Helv.* **1985**, *60*, 110–111. [[PubMed](#)]
81. Yu, D.G.; Wang, X.; Li, X.Y.; Chian, W.; Li, Y.; Liao, Y. Electrospun Biphasic Drug Release Polyvinylpyrrolidone/Ethylcellulose Core/Sheath Nanofibers. *Acta Biomater.* **2013**, *9*, 5665–5672. [[CrossRef](#)] [[PubMed](#)]
82. Liu, H.; Jiang, W.; Yang, Z.; Chen, X.; Yu, D.-G.; Shao, J. Hybrid Films Prepared from A Combination of Electrospinning and Casting for Offering a Dual-Phase Drug Release. *Polymers* **2022**, *14*, 2132. [[CrossRef](#)] [[PubMed](#)]
83. Wang, M.; Li, D.; Li, J.; Li, S.; Chen, Z.; Yu, D.-G.; Liu, Z.; Guo, J.Z. Electrospun Janus Zein–PVP Nanofibers Provide a Two-Stage Controlled Release of Poorly Water-Soluble Drugs. *Mater. Des.* **2020**, *196*, 109075. [[CrossRef](#)]
84. Li, C.-Q.; Wang, Y.-C.; Shen, S.-Q.; Zhang, Y.-L.; Zhao, J.-Q.; Zou, W.-B.; Ge, R.-L. Effects of Exercise by Type and Duration on Quality of Life in Patients with Digestive System Cancers: A Systematic Review and Network Meta-Analysis. *J. Sport Health Sci.* **2022**, *1*. [[CrossRef](#)]
85. Li, C.; Wang, J.; Deng, C.; Wang, R.; Zhang, H. Protocol for Atmospheric Water Harvesting Using in Situ Polymerization Honeycomb Hygroscopic Polymers. *STAR Protocols* **2022**, *3*, 101780. [[CrossRef](#)]
86. Xie, D.; Zhou, X.; Xiao, B.; Duan, L.; Zhu, Z. Mucus-Penetrating Silk Fibroin-Based Nanotherapeutics for Efficient Treatment of Ulcerative Colitis. *Biomolecules* **2022**, *12*, 1263. [[CrossRef](#)]
87. Castillo-Henríquez, L.; Castro-Alpízar, J.; Lopretti-Correa, M.; Vega-Baudrit, J. Exploration of Bioengineered Scaffolds Composed of Thermo-Responsive Polymers for Drug Delivery in Wound Healing. *Int. J. Mol. Sci.* **2021**, *22*, 1408. [[CrossRef](#)]
88. Sivan, M.; Madheswaran, D.; Valtera, J.; Kostakova, E.K.; Lukas, D. Alternating Current Electrospinning: The Impacts of Various High-Voltage Signal Shapes and Frequencies on the Spinnability and Productivity of Polycaprolactone Nanofibers. *Mater. Des.* **2022**, *213*, 110308. [[CrossRef](#)]
89. Liu, H.; Dai, Y.; Li, J.; Liu, P.; Zhou, W.; Yu, D.G.; Ge, R. Safe, Fast and Convenient Delivery of Fluidextracts Liquorice through Electrospun Core-Shell Nanohybrids. *Front. Bioeng. Biotechnol.* **2023**, *11*, 1172133. [[CrossRef](#)]
90. Hsiung, E.; Celebioglu, A.; Kilic, M.E.; Durgun, E.; Uyar, T. Fast-Disintegrating Nanofibrous Web of Pullulan/Griseofulvin-Cyclodextrin Inclusion Complexes. *Mol. Pharm.* **2023**, *20*, 2624–2633. [[CrossRef](#)]
91. Wu, Y.; Li, Y.; Lv, G.; Bu, W. Redox Dyshomeostasis Strategy for Tumor Therapy Based on Nanomaterials Chemistry. *Chem. Sci.* **2022**, *13*, 2202–2217. [[CrossRef](#)]
92. Zhao, P.; Li, H.; Bu, W. A Forward Vision for Chemodynamic Therapy: Issues and Opportunities. *Angew. Chem.-Int. Edit.* **2023**, *62*, e202210415.

93. Meng, Y.; Chen, L.; Chen, Y.; Shi, J.; Zhang, Z.; Wang, Y.; Wu, F.; Jiang, X.; Yang, W.; Zhang, L.; et al. Reactive Metal Boride Nanoparticles Trap Lipopolysaccharide and Peptidoglycan for Bacteria-Infected Wound Healing. *Nat. Commun.* **2022**, *13*, 7353. [[CrossRef](#)] [[PubMed](#)]
94. Tang, Z.M.; Wu, S.M.; Zhao, P.R.; Wang, H.; Ni, D.L.; Li, H.Y.; Jiang, X.W.; Wu, Y.L.; Meng, Y.; Yao, Z.W.; et al. Chemical Factory-Guaranteed Enhanced Chemodynamic Therapy for Orthotopic Liver Cancer. *Adv. Sci.* **2022**, *9*, 2201232. [[CrossRef](#)]
95. Chen, L.; Jiang, X.; Lv, M.; Wang, X.; Zhao, P.; Zhang, M.; Lv, G.; Wu, J.; Liu, Y.; Yang, Y.; et al. Reductive-Damage-Induced Intracellular Maladaptation for Cancer Electronic Interference Therapy. *Chem* **2022**, *8*, 866–879. [[CrossRef](#)]
96. Ge, R.; Ji, Y.; Ding, Y.; Huang, C.; He, H.; Yu, D.-G. Electrospun Self-Emulsifying Core-Shell Nanofibers for Effective Delivery of Paclitaxel. *Front. Bioeng. Biotechnol.* **2023**, *11*, 1112338. [[CrossRef](#)]
97. Abdul Hameed, M.M.; Mohamed Khan, S.A.P.; Thamer, B.M.; Rajkumar, N.; El-Hamshary, H.; El-Newehy, M. Electrospun Nanofibers for Drug Delivery Applications: Methods and Mechanism. *Polym. Advan. Technol.* **2023**, *34*, 6–23. [[CrossRef](#)]
98. Du, Y.; Yang, Z.; Kang, S.; Yu, D.-G.; Chen, X.; Shao, J. A Sequential Electrospinning of a Coaxial and Blending Process for Creating Double-Layer Hybrid Films to Sense Glucose. *Sensors* **2023**, *23*, 3685. [[CrossRef](#)]
99. Feng, Z.; Wang, K.; Liu, Y.; Han, B.; Yu, D.-G. Piezoelectric Enhancement of Piezoceramic Nanoparticle-Doped PVDF/PCL Core-Sheath Fibers. *Nanomaterials* **2023**, *13*, 1243. [[CrossRef](#)]
100. Isaacoff, B.P.; Brown, K.A. Progress in Top-Down Control of Bottom-Up Assembly. *Nano Lett.* **2017**, *17*, 6508–6510. [[CrossRef](#)] [[PubMed](#)]
101. Martins, L.M.; Fraga, G.N.; Pellá, M.C.G.; Pinto, F.A.C.; de Souza, F.; Neto, J.C.; Rossin, A.R.S.; Caetano, J.; Dragunski, D.C. Poly(1-vinylpyrrolidone-co-vinyl-acetate)-based electrospun dissolvable nanofibrous film for quercetin administration. *Process Biochem.* **2022**, *122*, 8–15. [[CrossRef](#)]

**Disclaimer/Publisher's Note:** The statements, opinions and data contained in all publications are solely those of the individual author(s) and contributor(s) and not of MDPI and/or the editor(s). MDPI and/or the editor(s) disclaim responsibility for any injury to people or property resulting from any ideas, methods, instructions or products referred to in the content.